# Electron-loss cross sections for fast, excited He atoms in $H_2$

E. Horsdal Pedersen
*Institute of Physics, University of Aarhus, DK 8000 Aarhus, Denmark*
(Received 26 December 1973)

By means of an optical detection technique, the electron-loss cross sections for He atoms in the excited states $3\,^3P$, $4\,^3S$, $4\,^1S$, $5\,^3S$, and $5\,^1S$ have been measured in $H_2$ in the energy range 8–160 keV. These cross sections are compared to theoretical cross sections derived by means of the classical impulse approximation of Bates and Walker. In agreement with this theory, the present electron-loss cross sections are found to depend very little on the binding energy and the specific quantum state of the weakly bound electron being removed. Further, they are approximately equal to the total electron-scattering cross section taken at the same impact velocity, as also predicted by the mentioned theory.

## I. INTRODUCTION

Recently several experimental papers concerned with destruction cross sections for fast excited atoms in various gases have been published. Gilbody and co-workers,[1,2] Miers and Anderson,[3] Tawara,[4] Dose and Gunz,[5] and Hughes and Choe[6] measured the electron-loss cross section for metastable helium and hydrogen atoms in various gases. Gilbody *et al.*[2] and Krotkov *et al.*[7] measured the total quenching cross section for metastable hydrogen, while Edwards and Thomas[8] and Hughes and Kisner[9] measured the same quantity for the $3s$ state of hydrogen. These cross sections were discussed in terms of the theoretical work of Bates and Walker,[10] who estimated the electron-loss cross section for weakly bound electrons on atoms, but the loss cross sections for the different excited states studied experimentally were not compared, although similarities between them are predicted by theory.

The Bates-Walker theory has also been applied in this laboratory to the cross section for electron loss from ground-state lithium.[11] In this work it was concluded that although the agreement between the Bates-Walker theory and the experimental results for ground-state lithium, metastable helium, and metastable hydrogen is fairly good in each individual case, experimental uncertainties imply that no final conclusion could be drawn about finer details, such as the dependence of the loss cross section on binding energy.

In order to investigate this aspect of the problem in more detail, an experiment was set up which allowed the measurement of electron-loss cross sections for fast excited helium atoms in the $3\,^3P$, $4\,^3S$, $4\,^1S$, $5\,^3S$, and $5\,^1S$ states by the same technique. The energy ranged from 8 to 160 keV, and the target gas was $H_2$.

## II. EXPERIMENTAL PROCEDURE

The measurements were performed at two accelerators. An isotope separator covered the energy range 8–80 keV, and a heavy-ion accelerator covered the range 60–160 keV. Both accelerators are equipped with universal ion sources and mass-separation magnets with dispersions of $1264\Delta M/M$ mm in the focal plane. The current of $He^+$ entering the experimental setup was typically of the order of a few $\mu$A.

The experimental arrangement is shown schematically in Fig. 1. The monoenergetic mass-analyzed beam of $He^+$ ions was partially neutralized in a thick He neutralizer and subsequently charge analyzed by means of a set of electrostatic deflection plates. The neutral-beam component proceeded into the 300-mm-long target-gas cell through a 1.0-mm entrance aperture. In the target-gas cell was a strong transverse electrostatic field (20 kV/cm) which ensured that the charged-beam particles were swept away from the neutral beam immediately upon formation. The remaining neutral particles left the target cell through a 2.0-mm aperture and were finally detected by a secondary-electron detector with the purpose of beam normalization, while a McPherson 218 spectrometer was set to monitor a certain He I line emitted by the neutral beam. The spectrometer was equipped with a 1200-lines mm grating blazed at 1500 Å and an EMI 6258 $S$ photomultiplier operated in the pulse-counting mode. The dark counting rate of the cooled photomultiplier was 2–3 per sec.

In this experiment, the relative intensity of the He I line normalized to the neutral-beam intensity, as given by the secondary emission detector, was measured as a function of pressure in the target-gas cell. An example of a measurement on the

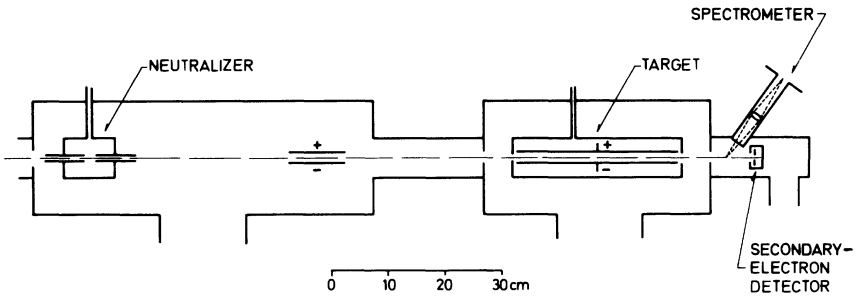


FIG. 1. Schematic diagram of the experimental arrangement.

$2\,^1P$-$4\,^1S$ line is shown in Fig. 2. In each run the normalization was checked by measuring half of the points, following a schedule of increasing pressures, and measuring the rest, lying in between, following a schedule of decreasing pressures. At each pressure both the total number of pulses from the photomultiplier and the time spent in counting these were recorded, making possible a correction for dark counts in the data analysis. In the typical example, shown in Fig. 2, this correction ranges from 10% at the lowest pressures to 3% at the highest ones. In order to eliminate the influence on the optical measurements of beam polarization as well as of instrumental polarization, the spectrometer viewed the beam at an angle of 54°, while the spectrometer slit made an angle of 45° to the plane through the ion beam and the light beam entering the spectrometer.[12]

The pressure in the gas cells was recorded by means of two Pirani gauges calibrated over the pressure range from $10^{-4}$ to $10^{-1}$ Torr against a capacitance manometer (Datametric 1038). The calibration was checked by a McLeod gauge (Consolidated Vacuum Corporation, type GM-100A).

## III. EXPERIMENTAL MEASUREMENTS

### A. Interpretation

In order to interpret the light-intensity-vs-pressure curves in terms of cross sections, it is necessary to consider the differential equations which connect these quantities:

$$\frac{dI_{0*}(R)}{dR} = -\left[\left(\sigma_{0*_1} + \sum_i \sigma_{0*_i}\right)N + \frac{1}{v\tau}\right] I_{0*}(R) + \sum_i \left(\sigma_{i0*}N + \frac{A_{i0*}}{v}\right) I_i(R)\,. \qquad (1)$$

$I_{0*}$ and $I_i$ are the respective intensities of neutral particles in the excited state being investigated and in the quantum state $i$. $\sigma_{0*_1}$ is the electron-loss cross section for the state $0^*$. $\sum_i \sigma_{0*_i}$ is the sum over all excitation and deexcitation cross sections from the investigated state $0^*$ to all other neutral states $i$, while $\sum_i \sigma_{i0*}$ is the corresponding sum over all cross sections from other excited states $i$ to the one being investigated, $0^*$. $R$ is the depth in the target-gas cell and $N$ the gas density. $v$ is the beam velocity, $\tau$ the lifetime of the excited state $0^*$, and $A_{i0*}$ the transition probability per second from state $i$ to state $0^*$.

By ignoring all excited states other than the one under investigation (an approximation which will later be discussed in more detail), Eq. (1) is reduced to

$$\frac{dI_{0*}(R)}{dR} = -\left(\sigma_{0*_1}N + \frac{1}{v\tau}\right) I_{0*}(R) + \sigma_{00*} N I_0(R)\,, \qquad (2)$$

where $I_0$ is the intensity of particles in the ground state and $\sigma_{00*}$ is the cross section for excitation from the ground state to the considered excited state.

In the same approximation, the intensity of ground-state neutrals is given by

$$I_0(R) = I_0(0)\exp(-\sigma_{0_1}NR)\,,$$

where $\sigma_{0_1}$ is the electron-loss cross section for the ground state.

Equation (2) can be solved analytically with this expression for $I_0(R)$. The solution is

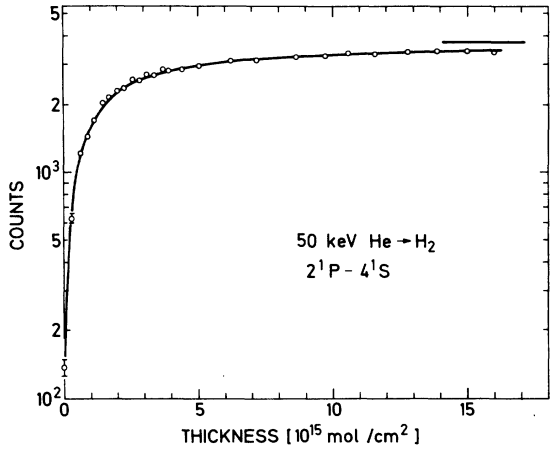


FIG. 2. Typical example of light-intensity vs target-thickness data together with the best least-squares fit of Eq. (3) to these. The asymptotic value of Eq. (3) is indicated. The goodness-of-fit parameter was in this case 0.98.

$$I_0*(R) = I_0*(0)\left[(1-f)\exp\left(-\sigma_0*_1 NR - \frac{R}{v\tau}\right) + f\exp(-\sigma_{01}NR)\right],$$

where

$$f = \frac{I_0(0)}{I_0*(0)}\frac{\sigma_{00}*N}{(\sigma_0*_1 - \sigma_{01})N + (1/v\tau)}.$$

With the special normalization used in this experiment (which does not correspond to a constant incoming, but rather to a constant emerging, intensity), the following expression is found for the measured light intensity $I_0'*$ versus target thickness $\mu = NL$, where $L$ is the length of the gas cell,

$$I_0'*(\mu) = K\left[[1-f(\mu)]\exp\left(-(\sigma_0*_1 - \sigma_{01})\mu - \frac{L}{v\tau}\right) + f(\mu)\right], \tag{3}$$

where

$$f(\mu) = \frac{I_0}{I_0*}\frac{\sigma_{00}*\mu}{(\sigma_0*_1 - \sigma_{01})\mu + (L/v\tau)}$$

and $K$ is a constant of proportionality.

The unknown parameters in Eq. (3) are $\sigma_0*_1$, $(I_0/I_0*)\sigma_{00}*$, and $K$. These were found by adjusting Eq. (3) to the experimental data by means of an iterative least-squares-fitting routine. The fully drawn curve in Fig. 2 is the result of such a fit. The lifetimes used for the investigated excited states are the mean values of the experimental results published in Refs. 13 and 14. They are 111 nsec for the $3\,^3P$ state, 66 nsec for the $4\,^3S$ state, 85 nsec for the $4\,^1S$ state, 105 nsec for the $5\,^3S$ state, and 133 nsec for the $5\,^1S$ state.

The strong electrostatic field in the target-gas cell, however, can give rise to a shortening of these lifetimes due to Stark mixing. The effect is strongest for the $5\,^1S$ state, which under the action of the electric field mixes with the adjacent short-lived $5\,^1P$ state. According to Bethe and Salpeter[15] the ratio between the strengths of the $1\,^1S$-$5\,^1S$ and $1\,^1S$-$5\,^1P$ transitions will be about equal to the ratio between the Stark-effect energy shift of the $5\,^1S$ level and the energy separation between the $5\,^1S$ and $5\,^1P$ states. At 20 kV/cm a Stark-effect energy shift of 1.2 $cm^{-1}$ is found for the $5\,^1S$ state and an energy separation of 280 $cm^{-1}$ between the $5\,^1P$ and $5\,^1S$ levels. Using the transition probability of $1.3\times10^8$ $sec^{-1}$ for the $1\,^1S$-$5\,^1P$ transition, a transition probability of about 5.7 $\times10^5$ $sec^{-1}$ for the $1\,^1S$-$5\,^1S$ transition is thus found. Adding this to the field-free transition probabilities for the $5\,^1S$ state lowers the lifetime of this state by about 7% to 124 nsec. While the neglect of this Stark-effect quenching may introduce a systematic error in the determination of the electron-loss cross section for the $5\,^1S$ state of about 7%, the cross sections being too low, it is completely negligible for the other investigated states.

### B. Discussion of interpretation

In Sec. III A the effect of all excited states other than the one being investigated was ignored. The influence of these is twofold. There will be contributions from collisional excitation and deexcitation as well as cascade contributions. In order to get a theoretical estimate of the relative importance of these contributions, they were calculated for the H $(4s)$ + H system at the representative impact velocity of 10 keV/amu, using the theoretical excitation and deexcitation cross sections of Pomilla[16] and the theoretical electron-loss cross section for the H $(2s)$ + H system given by Bell *et al.*[17] These cross sections are all calculated in the first Born approximation (exchange neglected). It is assumed that the Born loss cross section for the $4s$ state is relatively close to that for the $2s$ state. The transition probabilities used were those for the triplet spectrum of He I taken from the tabulation of Wiese *et al.*[18]

Because the investigated excited helium states are hydrogenlike, it is reasonable to assume that the hydrogen-hydrogen system mentioned will given a good estimate of the relative importance of the various collision processes for the states under investigation here.

The collisional and cascade contributions are

$$-\left(\sum_f \sigma_{4s,f}I_{4s} - \sum_f{}' \sigma_{f,4s}I_f\right)N + \sum_f \frac{A_{f,4s}}{v}I_f, \tag{4}$$

where the prime indicates that the ground state is omitted in this sum.

This quantity should be compared to the remaining terms of Eq. (1),

$$-\left(\sigma_{4s,1}N + \frac{1}{v\tau}\right)I_{4s} + \sigma_{1s,4s}NI_{1s}, \tag{5}$$

which were the only ones used in deriving Eq. (3).

The relative populations of the excited states are estimated in the following way: In the single-collision region, one finds

$$I_i = \sigma_{1s,i}I_{1s}Nv\tau[1 - e^{R/v\tau}],$$

which gives the following approximate result for the states considered here lying close to each other and all having lifetimes of the same order of magnitude:

$$\frac{I_i}{I_j} = \frac{\sigma_{1s,i}}{\sigma_{1s,j}}. \tag{6}$$

Correspondingly, for $N$ going to infinity, Eq. (1) reduces to

$$\frac{dI_i(R)}{dR} = -\left(\sigma_{i,1} + \sum_j \sigma_{i,j}\right)NI_i(R) + \sum_j \sigma_{j,i}NI_j(R)$$

and $I_i$ will be given by

$$I_i(R) = F_i \exp(-\sigma_{01} N R),$$

where $F_i$, being independent of $R$, measures the relative amount of neutrals in the state $i$.

These two equations lead to

$$\sum_i \sigma_{j,i} F_j - \sum_j \sigma_{i,j} F_i - (\sigma_{i,1} - \sigma_{01}) F_i = 0,$$

which is formally solved by

$$F_i = \frac{\sum_j \sigma_{j,i} F_j}{\sigma_{i,1} - \sigma_{01} + \sum_j \sigma_{i,j}}$$

$$\simeq \frac{\sigma_{1s,i} F_{1s}}{\sigma_{i,1}} + \frac{\sum_j' \sigma_{j,i} F_j}{\sigma_{i,1}},$$

where, in the last step, it is assumed that $\sigma_{i,1} \gg |\sum_j \sigma_{ij} - \sigma_{01}|$.

By further assuming that the first term in this expression is dominating, an explicit iterative solution is finally obtained:

$$F_i = \left( \frac{\sigma_{1s,i}}{\sigma_{i,1}} + \sum_j \frac{\sigma_{1s,j}\sigma_{j,i}}{\sigma_{i,1}^2} + \ldots \right) F_{1s}. \tag{7}$$

Keeping only the first term of this expression one finds approximately the same expression as before [Eq. (6)] for the relative population of excited states.

This expression is therefore adopted for the whole pressure range. By inserting it into Eq. (4), one arrives at the expression

$$-\sigma_{4s,1s} NR - \sum_f' \sigma_{4s,f} \left(1 - \frac{\sigma_{1s,f}}{\sigma_{1s,4s}}\right) NR + \sum_f \frac{A_{f,4s}}{v} R \frac{\sigma_{1s,f}}{\sigma_{1s,4s}}$$

for the collisional and cascade contributions, which should be compared to

$$-\sigma_{4s,1} NR - \frac{R}{v\tau}.$$

Using the cross sections and transition probabilities mentioned earlier, the latter two expressions reduce to

$$+4.0 \times 10^{-2} (\pi a_0^2 NR) + 1.4 \times 10^{-2}$$

and

$$-1.5 \pi a_0^2 NR - 3.3,$$

respectively. Furthermore, Eq. (7) becomes

$$I_{4s} = (2.6 \times 10^{-3} + 5.1 \times 10^{-5} + \ldots) I_{1s},$$

which shows that double processes are relatively insignificant for this state.

On the basis of these estimates, it was concluded that the influence of other excited states on the one under investigation is negligible over the whole pressure range.

This conclusion is supported by various experimental facts. First of all, the approximate expression (3) could be fitted very well to the experimental light-intensity-vs-pressure curves. The goodness of fit, which is defined as the ratio between the number of degrees of freedom in the fit and the final square sum, was not significantly different from 1 in any of the measurements published here. According to the least-squares theory, this is the ideal value for normally distributed data. Second, the influence of cascades was investigated by measuring the light intensity emitted from the $3\,^3P$, $4\,^3S$, and $4\,^1S$ states as a function of the distance from the gas cell for various gas pressures. The light intensity was, as expected, found to fall off without cascades in all these cases, following a single exponential decay. The lifetimes found from these measurements are $115 \pm 5$ nsec for $3\,^3P$, $65 \pm 3$ nsec for $4\,^3S$, and $84 \pm 7$ nsec for $4\,^1S$, in good agreement with other measurements of these lifetimes. As a final and more indirect test of the approximations made in Eq. (3), light-intensity-vs-pressure curves were measured for the $3\,^3P$ state for both incident neutral and singly charged helium without the attenuation field in the target-gas cell being turned on. The relevant equations describing these cases were solved,[8,9] neglecting excited states other

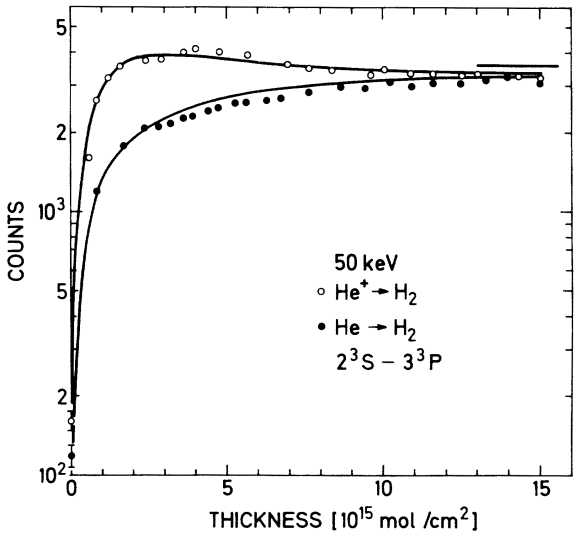


FIG. 3. Light-intensity vs target-thickeness data obtained without field attenuation in the target cell. The full-drawn curves are theoretical ones derived as explained in the text. The asymptotic value is indicated.

than the one under investigation as in Eq. (3), and the solutions were roughly fitted to the experimental data. The result is shown in Fig. 3. The only parameters that varied in the fit were the cross-section ratio $\sigma_{00}*/\sigma_{10}*$ and a constant of proportionality such as $K$ in Eq. (3). In this example $\sigma_{00}*/\sigma_{10}*=0.37$, a reasonable value which unfortunately has not been measured or estimated in the literature. The remaining parameters used are $\sigma_0*_1=1.6\times10^{-15}$ cm$^2$/mol, ground-state capture and loss cross sections as tabulated by Allison and Garcia-Munoz,[19] and the lifetime indicated earlier in this article. The fit is found to be reasonably good. In particular, the maximum in the case of $He^+$ is nicely reproduced by the theory.

Exchange reactions have been neglected until now, although Hughes and Kisner[9] have argued that electron capture by the singly charged core of the excited neutral particles can be a significant deexcitation mechanism. Its inclusion in the analysis will not change the form of Eq. (3). Only the interpretation of the derived cross sections has to be changed. They will be total-quenching rather than electron-loss cross sections. In the present case, however, the ratio of the capture cross section to the measured loss cross section is rather small, varying from 10% at low energies to 15% at high energies. In view of the approximations already made, this correction was neglected.

The geometry of the target-gas cell was such that only projectiles scattered through angles less than about 10 mrad would reach the detection region. The influence on the present results of elastic scattering out of this cone was estimated by calculating the integrated Rutherford cross section for scattering through angles larger than 10 mrad for He or H. At 10 keV this cross section is $0.82\pi a_0^2$ and it varies with energy as $E^{-2}$. The loss cross section per hydrogen atom for the excited states investigated here, being of the order of $8\pi a_0^2$, are thus at least an order of magnitude larger than these scattering cross sections. It was therefore concluded that elastic scattering does not have any significant influence on the present results, even at the lowest energies.

The spectrum of helium lines emitted by the beam after the gas cell contained strong $^1D$ and $^3D$ states besides the investigated $P$ and $S$ states. Unseccessful attempts were made to analyze intensity-vs-pressure curves for these states, using Eq. (3). The goodness-of-fit parameter

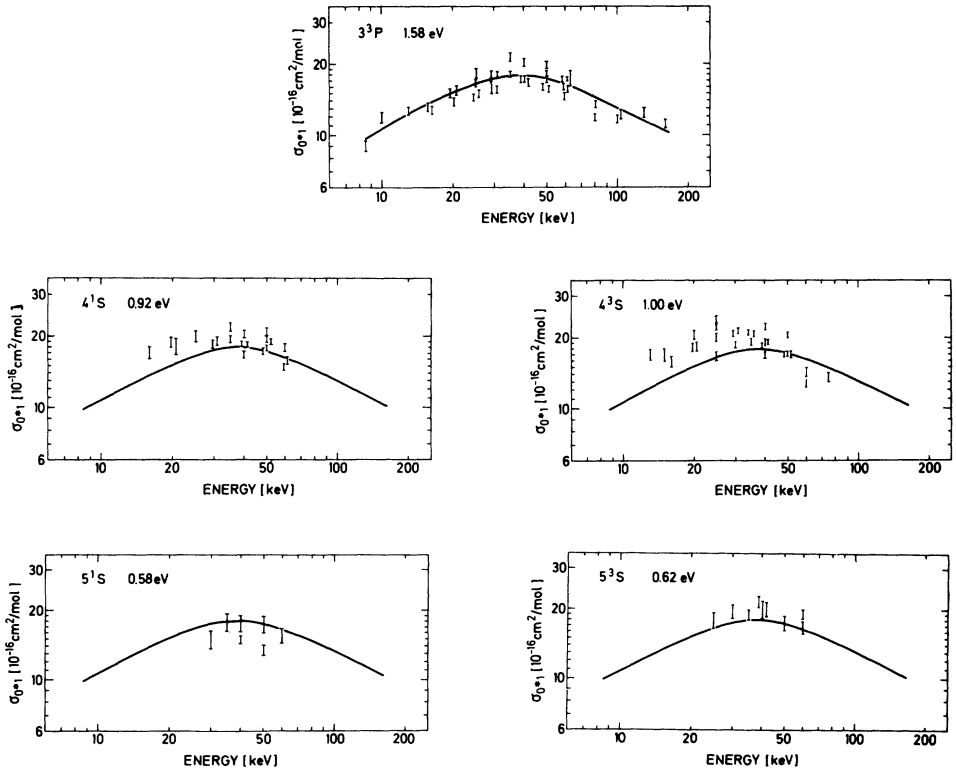


FIG. 4. Electron-loss cross sections in $H_2$ for various excited states of He. The ionization potentials are indicated. The full-drawn curve facilitating comparison is the same in all the figures.

turned out to be significantly different from 1 in all cases. Furthermore, the lifetime measurements for these states show that they are influenced by strong long-lived cascades. This shows experimentally that the approximations leading to Eq. (3) do not apply to $D$ states. The reason is that the states with high orbital angular momenta are mainly populated via excited $S$ and $P$ states [the second term of Eq. (7)]. No attempts were made to analyze the $D$-state results in terms of theoretical expressions more complicated than Eq. (3) and containing an excessive number of unknown parameters.

## IV. RESULTS AND DISCUSSION

Figure 4 shows the experimental results. The indicated errors are the ones estimated by the fitting routine, and they reflect the counting statistics in the individual measurements. The scatter of the points reflects the total statistical error, which is about ±15%. The possible systematic error, including the approximations made in Eq. (3), is believed to be less than 20%.

The present electron-loss cross sections are discussed in terms of the Bates-Walker theory, which is developed with the purpose of making it possible to estimate electron-loss cross sections for weakly bound electrons. According to this theory, the loss cross section for a given target gas depends on binding energy and impact velocity only. For small binding energies, the theory further predicts that the loss cross section is close to the total electron-scattering cross section taken at the same impact velocity and hence largely independent of binding energy.

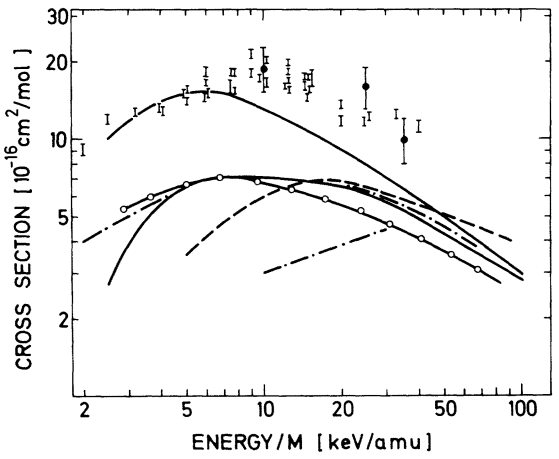


FIG. 5. Electron-loss cross sections in $H_2$ plotted against impact energy per atomic mass unit of the projectile. The solid upper curve represents the total experimental cross section for electron scattering in $H_2$ and the lower solid curve represents the theoretical Bates-Walker electron-loss cross section for He ($2\,^3S$). Experimental electron-loss cross sections are plotted as follows: Vertical error bars: He ($3\,^3P$), this experiment; error bars through full circles: H ($3s$), Ref. 9; dash-dot-dashed line: H ($2s$), upper curve, Ref. 5, lower curve, Ref. 2; dashed line: He ($2\,^3S$), Ref. 1; dash-circle-dashed line: Li, Ref. 11.

In Fig. 4, which shows all the measured loss cross sections, an average curve is drawn through the results for the $3\,^3P$ state. This curve is repeated on the plots for the other investigated states in order to facilitate comparison. Taking into account the experimental uncertainties discussed earlier, the present electron-loss cross sections are, in agreement with the Bates-Walker theory, found to be independent of binding energy as well as of the specific quantum state of the removed electron.

Figure 5 shows the electron-loss cross section for the $3\,^3P$ state together with the total experimental electron-scattering cross section[20] and the Bates-Walker cross section for metastable He ($2\,^3S$), as estimated by the present author[11] by means of the electron-scattering cross sections. Further, the figure includes the experimental cross sections for hydrogen in the $3s$ state, metastable helium, and ground-state lithium.

The agreement between the quenching cross sections for hydrogen atoms in the $3s$ state (binding energy 1.51 eV) and the present cross sections is good. This is also the case if the quenching mechanism discussed by Hughes and Kisner[9] is taken into account by subtracting the respective electron-capture cross sections from the ones plotted in Fig. 5. This agreement, which is in accord with the previous conclusion that the loss cross section for loosely bound electrons depends only weakly on binding energy, supports the absolute calibration used in the experiments.

At high velocities, the total experimental electron-scattering cross section is 40% smaller than the present electron-loss cross section, whereas at low velocities the two cross sections agree. In view of the uncertainties in the theoretical approximations leading to the Bates-Walker expression for the loss cross section, combined with the uncertainties in the experimental electron-scattering cross sections and the present cross sections, this disagreement, however, is not found to be significant.

The electron-loss cross sections for metastable hydrogen ($I = 3.4$ eV), metastable helium ($I = 4.8$ eV), and ground-state lithium ($I = 5.4$ eV) tend to cluster around the theoretical Bates-Walker cross section for $I = 4.8$ eV, again in qualitative agree-

ment with this theory. As mentioned earlier, however, the experimental uncertainties in these measurements render a closed comparison impossible.

Finally, it can be concluded that the electron-loss cross section in hydrogen for very weakly bound electrons is independent of the binding energy and the specific quantum state of the electron being removed. Further, the cross section is approximately equal to the total electron-scattering cross section taken at the same impact velocity. These conclusions are in agreement with the Bates-Walker theory.

ACKNOWLEDGMENT

The author wishes to express his gratitude to P. Hvelplund for valuable discussions in all phases of this work.

[1]H. B. Gilbody, K. F. Dunn, R. Browning, and C. J. Latimer, J. Phys. B 3, 1105 (1970).
[2]H. B. Gilbody, R. Browning, R. M. Reynolds, and G. I. Riddell, J. Phys. B 4, 94 (1971).
[3]R. E. Miers and L. W. Anderson, Phys. Rev. A 1, 819 (1970).
[4]H. Tawara, J. Phys. Soc. Japan 31, 236 (1971); J. Phys. Soc. Japan 31, 871 (1971).
[5]V. Dose and R. Gunz, J. Phys. B 5, 636 (1972).
[6]R. H. Hughes and S. S. Choe, Phys. Rev. A 6, 1413 (1972).
[7]R. V. Krotkov, F. W. Byron, J. A. Medeiros, and K. H. Yang, Phys. Rev. A 5, 2078 (1972).
[8]J. L. Edwards and E. W. Thomas, Phys. Rev. A 2, 2346 (1970).
[9]R. H. Hughes and H. Kisner, Phys. Rev. A 5, 2107 (1972).
[10]D. R. Bates and J. C. G. Walker, Planet. Space Sci. 14, 1367 (1966).
[11]E. Horsdal Pedersen and P. Hvelplund, J. Phys. B 6, 1277 (1973).
[12]P. N. Clout and D. W. O. Heddle, J. Opt. Soc. Am. 59, 715 (1969).
[13]K. A. Bridgett and T. A. King, Proc. Phys. Soc. Lond. 92, 75 (1967).
[14]A. L. Osherovich and Ya. F. Verolainen, Opt. Spectrosc. 24, 81 (1968).
[15]H. A. Bethe and E. E. Salpeter, *Quantum Mechanics of One- and Two-Electron Atoms* (Springer-Verlag, Berlin, 1957), Secs. 56 and 57.
[16]F. R. Pomilla, Astrophys. J. 148, 559 (1967).
[17]K. L. Bell, A. E. Kingston, and W. A. McIlveen, J. Phys. B 6, 1237 (1973).
[18]W. L. Wiese, M. W. Smith, and B. M. Glennon, *Atomic Transition Probabilities*, Natl. Bur. Std. Publ. No. NSRDS-NBS4 (U. S. GPO, Washington, D. C., (1966), Vol. 1.
[19]S. K. Allison and M. Garcia-Munoz, *Atomic and Molecular Processes*, edited by D. R. Bates (Academic, New York, 1962), p. 721.
[20]R. B. Brode, Rev. Mod. Phys. 5, 257 (1933).